



Experimental study of the superplastic and hot deformation mechanisms of a Ti-6Al-2Sn-4Zr-2Mo Titanium Alloy

Gen Yamane, Felantsoa Avotriniaina, Hiroyuki Imai, Longqiu Song, Vanessa Vidal, Hiroaki Matsumoto, Vincent Velay

► To cite this version:

Gen Yamane, Felantsoa Avotriniaina, Hiroyuki Imai, Longqiu Song, Vanessa Vidal, et al.. Experimental study of the superplastic and hot deformation mechanisms of a Ti-6Al-2Sn-4Zr-2Mo Titanium Alloy. Ti 2019 - The 14th world conference on titanium, Jun 2019, Nantes, France. 6 p., 10.1051/mateconf/202032111023 . hal-02384311

HAL Id: hal-02384311

<https://imt-mines-albi.hal.science/hal-02384311>

Submitted on 22 Oct 2020

HAL is a multi-disciplinary open access archive for the deposit and dissemination of scientific research documents, whether they are published or not. The documents may come from teaching and research institutions in France or abroad, or from public or private research centers.

L'archive ouverte pluridisciplinaire **HAL**, est destinée au dépôt et à la diffusion de documents scientifiques de niveau recherche, publiés ou non, émanant des établissements d'enseignement et de recherche français ou étrangers, des laboratoires publics ou privés.



Distributed under a Creative Commons Attribution 4.0 International License

Experimental study of the superplastic and hot deformation mechanisms of a Ti-6Al-2Sn-4Zr-2Mo Titanium Alloy

Gen YAMANE^{1,2}, Felantsoa AVOTRINIAINA^{1,2}, Hiroyuki IMAI², Longqiu SONG^{1,2}, Vanessa VIDAL¹, Hiroaki MATSUMOTO², Vincent VELAY¹.

¹Institut Clément Ader (ICA), Université de Toulouse, CNRS, IMT Mines Albi, UPS, INSA, ISAE-SUPAERO, Campus Jarlard, 81013 Albi CT Cedex 09, France.

² Department of Advanced Materials Science, Faculty of Engineering, Kagawa University, 2217-20 Hayashi-cho, Takamatsu, Kagawa 761-0396, Japan.

Abstract

To clarify the hot deformation characteristics of Ti alloys, flow behaviour, microstructural evolution and deformation mechanisms were investigated in a Ti-6Al-2Sn-4Zr-2Mo alloy with two initial microstructure: an ultra-fine grained (UFG) and a fine-grained (FG) microstructure ($d_{\alpha}=0,8\ \mu\text{m}$ and $d_{\alpha}=3\ \mu\text{m}$ respectively) by isothermal interrupted tensile tests, SEM observations and through electron back scatter diffraction experiments.

Depending on the test conditions and on the initial α grain size, the flow behaviour can exhibit steady state flow and/or hardening and/or softening. The microstructure and texture evolutions have been studied mainly by using electron backscatter diffraction (EBSD) technique and SEM observations. They evidenced in particular the occurrence of α grains growth as well as dynamic recrystallization (DRX).

The different flow behaviour associated to the microstructure evolution is shown and discussed to clarify the main deformation mode that could be assume to occur depending on the microstructure, the temperature and the strain rate.

1. Introduction

Because of its superior high-temperature properties compared to the popular Ti-6Al-4V alloy, Ti-6Al-2Sn-4Zr-2Mo (Ti-6242) alloy can be used in aerospace structures requiring creep resistance at elevated temperatures. This near-alpha titanium alloy shows also interesting capabilities to be superplastically formed, i.e., to reach high elongation without necking under specific conditions of temperature ($T \sim 0.5T_{\text{melting}}$), strain rate ($\dot{\epsilon} \leq 10^{-3}\ \text{s}^{-1}$) and microstructure (fine and stable grain size) [1].

One of the main challenges of superplastic forming, known to allow the production of complex part geometries, is to decrease its costs by reducing the forming temperature and/or its time. However SPF of the Ti6242 alloy requires higher temperature than for the Ti-6Al-4V alloy. So to improve the process with the objective of reducing the cost, it appears important to understand more deeply the phenomena and mechanisms involved as well as optimizing the microstructure (as grain refinement).

Superplasticity is mainly explained by grain boundary sliding (GBS) associated with different accommodation mechanisms such as dynamic recrystallization, grain growth, slip in grains, grain boundary migration, diffusion, phase transformation etc [2-3]. All of these mechanisms may depend on the temperature, the strain rate but also on the initial alloy microstructure (preferred orientation, size and shape of the grains, phase fraction and distribution). This implies that a strong interaction between the microstructure evolution and hot deformation behaviour exists during hot deformation process.

We are currently studying the deformation behaviour, of a Ti6242 alloy under different hot deformation conditions (temperature from 600°C to 960°C and strain rate between 10^{-2}s^{-1} and 10^{-4}s^{-1}) and for different initial α grain sizes (from 0.8 μm to 5 μm) ; the final objectives being (i) to understand the effect of the initial microstructure on the hot deformation behaviour and (ii) to be able to propose adequate thermo-mechanical behaviour models taking into account microstructural considerations [4-7].

In this context, this paper focuses on the interaction between the microstructure evolution and the hot deformation and superplastic behaviour of a Ti6242 alloy sheets characterized by different initial microstructure: ultra-fine grained (UFG) and fine grained (FG) samples have respectively an α nodule size of around $d_{\alpha}=0,8\ \mu\text{m}$ and $d_{\alpha}=3\ \mu\text{m}$. Interrupted tensile tests carried out at different temperatures (from 650°C to 850°C) reveal different flow behaviour. Results of the associated microstructural evolution are shown and discussed in terms of mechanisms of hot deformation.

2. Materials and experimental procedure

2.1 Materials

The material investigated in this study is a Ti6242 alloy titanium in the shape of 4 mm thick sheet with a chemical composition (in wt%) of 6.02 Al, 2.05 n, 4.1 Zr, 2.01Mo, 0.09 Si, 0.1 O, 0.02 N, and balance Ti. The transus beta is $T_{\beta}=995^{\circ}\text{C}$.

The initial microstructure consists of equiaxed nodules of the hexagonal α phase, with a mean diameter of approximately 3 μm , separated by a thin layer of the bcc β phase. The β phase fraction, which is around $V_{\beta} = 11\%$, can be considered as the equilibrium value of the phase fraction (figure 1).

By applying different thermo-mechanical treatment on this initial material, other microstructure characterized each by different α grain size, morphology and phase fraction were obtained (see references [8-9] and [10] for details concerning respectively the process and its application to Ti6242 alloy). This work focuses on the results obtained on two microstructures ($d_{\alpha}=0.8\mu\text{m}$ (UFG), $d_{\alpha}=3\mu\text{m}$ (FG) as shown on figure 1).

The UFG sample is characterized by mainly equiaxed α nodules. The volume fraction of β is around 2,8%. This low value of β phase fraction, compared to the FG sample, revealed that this UFG has an initial “metastable” microstructure due to the thermo-mechanical treatment applied on it.

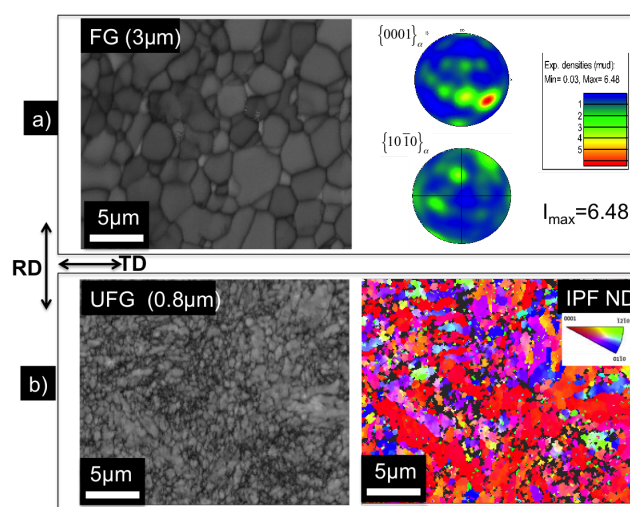


Figure 1: initial microstructure of (a) the fine grained (band contrast images and pole figures from EBSD data) and (b) the ultra-fine grained Ti6242 (band contrast images and IPF ND maps from EBSD data) (RD, TD and ND are respectively the Rolling, Transverse and Normal directions of the sheet)

2.2 Tensile tests

Tensile tests along the rolling direction are performed in a wide temperature range (650°C - 920°C) and in a strain rate range of 10^{-2}s^{-1} and 10^{-4}s^{-1} . Most of the tensile tests were performed at the Kagawa University in air atmosphere (a specific coating was used on the surface to minimize some oxidation phenomenon). For FG1 samples (initial α grain size of 3 μm), the test at 730°C and 840°C were conducted at ICA-IMT Mines Albi [11]. Note that in this case Argon atmosphere was used. In addition, interrupted tensile tests were performed on UFG and FG samples at respectively 700°C , 800°C , 900°C and 700°C , 730°C , 800°C , 840°C , 900°C .

2.3 microstructural analyses

For microstructural analyses, the deformed specimens were sectioned parallel to tensile axis (RD/TD surface). The microstructure was characterized by scanning electron microscopy (SEM) in the back-scattered electron (BSE) mode and by electron backscattered diffraction analysis (Oxford –HKL EBSD detector). The specimens for SEM observations and EBSD were mechanically polished using standard metallographic procedure (more details in [10]).

3. Results and discussion

Tensile tests confirm the occurrence of a superplastic flow at lower temperature and at higher strain rate for the samples with the smallest α grain size (UFG).

At low temperature (650°C - 730°C) and at high strain rate, the flow behaviour of the UFG materials seems to be mainly governed by dislocations activity. On the contrary, at low strain rate (10^{-4}s^{-1}), a lower flow stress and a higher elongation

associated with a steady state flow characteristic of a superplastic flow is obtained (figure 2). SEM and EBSD reveal, for this lower strain rate, a slight α grain growth and a randomization of the initial α grain orientation. Moreover an increase of the β phase fraction (from around 3% to 11%) is noticed for all testing conditions. Additionally, interrupted tensile tests carried out at 700°C and for low strain rate, reveal the occurrence of a partial dynamic recrystallization (DRX) [10] that can be related, in the strain-stress curve, to the slight softening observed before the stationary behaviour. So for the UFG material the higher elongation can be due, at initial stage of deformation, to a dislocation activity accompanied by the dissolution of the α phase as well as a partial DRX. Then, at intermediate stage of deformation and till the fracture, grain boundary sliding seems to be the dominant deformation mode in particular at lower strain rate.

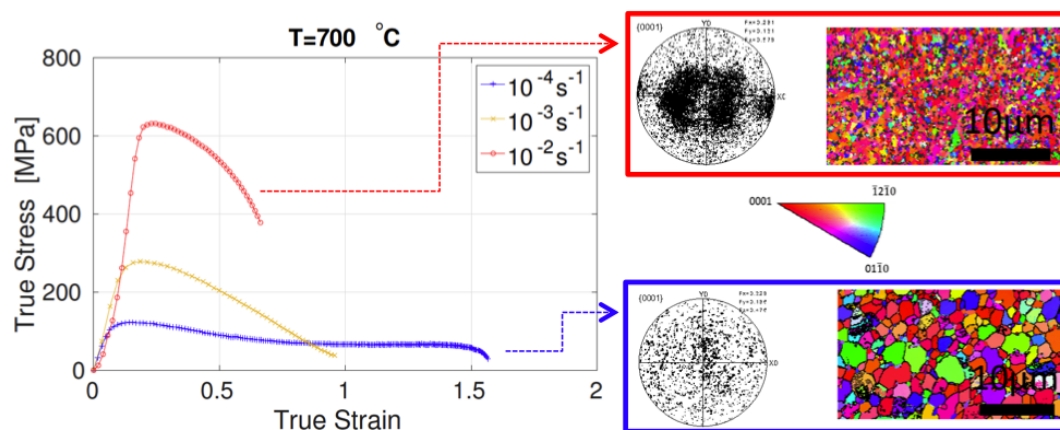


Figure 2: true stress-true strain curves, $\{0001\}_{\alpha}$ pole figures and EBSD ND orientation images of the UFG material obtained at 700°C for different strain rate.

At 700°C, for the FG material, higher flow stress (for the lower strain rate) as well as a lower elongation (around 0.4 of true strain against around 1 and 1.6 for the UFG sample at 10^{-3} s^{-1} and 10^{-4} s^{-1}) is obtained (figure 3).

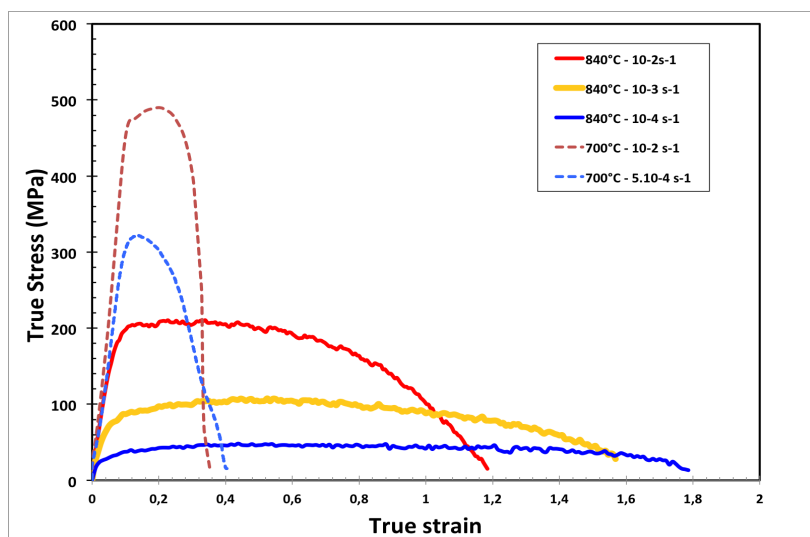


Figure 3: true stress-true strain curves obtained for the FG material at 700°C and 840°C for different strain rate.

Even if no α grain growth is shown between the initial state and after the failure, interrupted tensile tests indicate the formation of few subgrains at intermediate stage of the deformation (in particular for the lower strain rate). Finally before and after tensile test, the α grains are still equiaxed and with a size around 3 μm (figure 4). A texture characterized by basal poles $\{0001\}_{\alpha}$ tilted by around $\pm 80^\circ$ from the normal direction towards almost the transverse direction is revealed for intermediate and low strain rate (mainly at 10^{-3} s^{-1}). This suggests that in the FG sample dislocations sliding might be the dominant mode of deformation at temperatures around 700°C-730°C.

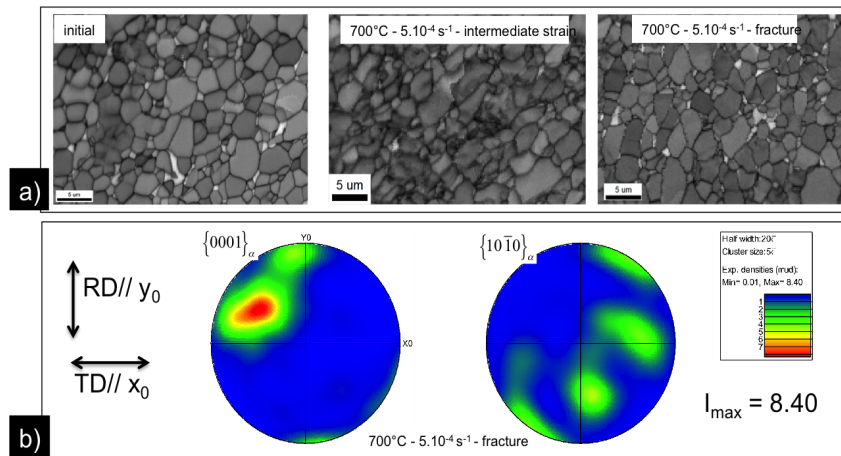


Figure 4: (a) band contrast images showing the microstructure of the FG material tested at 700°C with a strain rate of 5.10^{-4} s^{-1} and for various strain (from initial to the failure) (b) pole figures obtained for the FG material after tensile test (700°C / 5.10^{-4} s^{-1})

So at low temperature (650°C-730°C), the UFG sample has lower flow stress as well as a higher elongation compared to the FG. The mechanisms allowing this behaviour are supposed to be linked to (i) the low α grain size which favour the grain boundary sliding and (ii) the dynamic precipitation of the beta phase into the metastable microstructure which can act as an additional accommodation mechanism [10,12]. Indeed, in the case of non-equilibrium interfaces, the GBS can be accommodated and controlled first by the diffusion phenomenon that could promote the dissolution of the α phase. Then with the increase of the β phase fraction, GBS can go on but by being accommodated by other mechanisms (dislocation sliding into the β phase and/or diffusion).

In comparison, for the FG sample, mainly dislocation activity (into the α phase) associated to DRX or dynamic recovery seems to occur. It can be note that for low strain rate, GBS can be also initiated at late stage of deformation, as the α grains tend to slightly randomize.

At higher temperature (800°C-850°C), even if the UFG sample still exhibits higher elongation than the FG sample, the stress-strain curves as well as the microstructure evolution are different from the ones obtained at 700°C-730°C. In the UFG sample a α grain growth is clearly observed for all strain rate. At the lower strain rate, this feature is particularly significant and might induce the strain hardening observed during the tensile test (figure 5).

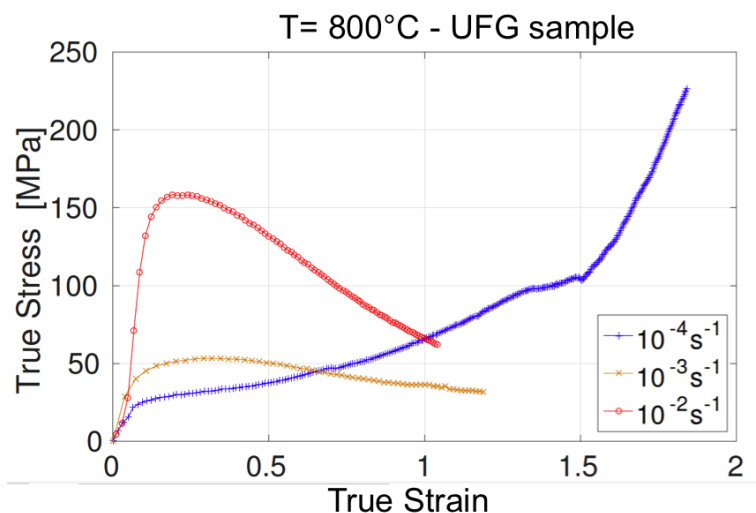


Figure 5: true stress-true strain curves obtained for the UFG material at 800°C and for different strain rate.

By increasing the strain rate (from 10^{-3} s^{-1} and 10^{-2} s^{-1}), the flow stress increases and the elongation decreases. Moreover, after the initial peak of stress, a continuous strain softening is observed at 10^{-2} s^{-1} while an almost steady state behaviour occurs at 10^{-3} s^{-1} . In these UFG samples, in addition to a α grain growth, a randomization of the α grain orientation, and an increase of the β phase fraction were revealed [10]. It can be thus supposed that GBS might be the dominant mechanisms of deformation accommodated by the dynamic dissolution of the α phase for the benefit of the β phase. For low strain rate, GBS should be less involved due to the noticeable α grain growth leading to a strain hardening.

On the contrary to the UFG sample, in the FG sample, the α grain size before and after tensile tests at 800°C-840°C, seems to have a tendency to (i) increase for lower strain rate (more evident at 840°C with a final α grain size around 5 μm) and (ii) slightly decrease for higher strain rate (around 2 μm) (figure 6). Interrupted tensile tests reveal the formation of subgrains (probably promoted by dislocation activity) for higher strain rate, while for the lower strain rate (10^{-4} s^{-1}) the α grains size tends to increase gradually with the strain. Moreover, while a strong texture is obtained after tensile tests at 10^{-2} s^{-1} , by decreasing the strain rate the grains orientation of α tends to randomize (figure 6). In addition the retention of the initial equiaxed shape is noticed whatever the strain rate. So around 800°C-840°C, mechanisms that could occur are : (i) intra-granular dislocations activity leading maybe to a DRX occur at high strain rate while (ii) GBS assisted by grain boundary motion and so by a grain growth at low strain rate.

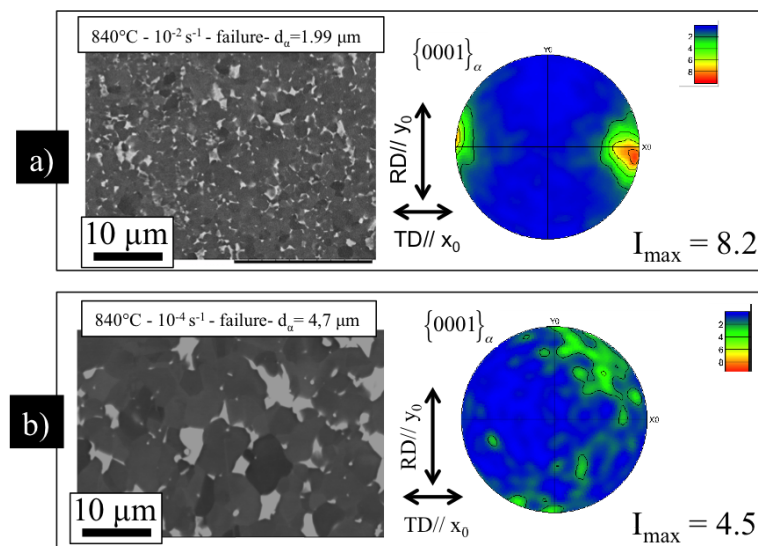


Figure 6: SEM-BSE images and $\{0001\}_{\alpha}$ pole figures of the FG material after tensile tests at 840°C and for two different strain rates :
(a) 10^{-2} s^{-1} and (b) 10^{-4} s^{-1} .

So for temperatures in the range of 800-850°C, classical superplastic mechanisms (GBS) accommodated by diffusion (and thus by the increase of the β phase fraction) as well as α grain growth, occurs in UFG sample (GBS). On the other hand, in the FG sample the dominant deformation mode seems to be linked to the activity of dislocations that could promote the occurrence of dynamic recovery and/or DRX into the α phase (for high strain rate). Then, for low strain rate and from intermediate elongation, GBS can occur as suggested by the increase of the fraction of randomly oriented α grains. Moreover for this lower strain rate GBS seems to be accomodated by a sligh grain growth until the failure.

4. Conclusions

The influence of the initial microstructure ($d_{\alpha}=0.8\mu\text{m}$ and $d_{\alpha}=3\mu\text{m}$) on the flow behaviour of the Ti6242 alloy at temperature ranging from 700°C to 850°C and for a strain rate between 10^{-2} s^{-1} and 10^{-4} s^{-1} was shown.

It is confirmed that, the refinement of the microstructure, enables the improvement of the superplastic properties (higher ductility) of the Ti6242 alloy at lower temperature and for higher strain rate. Indeed whatever the testing conditions, UFG samples show lower flow stress and higher elongation than the FG samples. Moreover, it was found from SEM and EBSD analysis, that for each testing conditions different mechanisms of plasticity can be involved and their contribution may evolve throughout the deformation.

The experimental results suggest that not only the α grain refinement but also the dissolution of the α phase may enhance the elongation of UFG material at lower temperature and higher strain rate : the mechanism of GBS accommodated by the precipitation of β seems to be the main deformation mechanisms for the UFG sample. Meanwhile, it is worth noticing that for temperature higher than 800°C and for low strain rate, this starting microstructure tends to promote an important α grain growth and so a strain hardening which might be problematic for industrial applications.

In comparison, the FG material shows only interesting elongation at temperature above 800°C and for low strain rate. It seems, from our results, that mainly intra-granular mechanisms as dislocation gliding accompanied or not by dynamic recovery or DRX might be involved throughout the plastic deformation of the FG sample. Nevertheless, the enhanced elongation, in particular for the lower strain rate, could be attributed to the contribution of GBS accomodated by grain growth. Additional experiments as well as a more detailed analysis of the interrupted tensile tests are still needed to clarify

the microstructural evolution throughout the hot deformation and so to propose improved thermo-mechanical models including some microstructural parameters (grain growth, DRX, recovery, texture evolution...).

5. **References**

- [1] E-L. Odenberger, R. Pederson, Mats Oldenburd, Mat. Sc. And Eng. A. 489 (2008) 158-168.
- [2] M. Ashby, R.Verrall, Acta Metall. 21 (1973) 149-163.
- [3] E. Alabort, P. Kontis, D. Barba, K. Dragnevski, and R. C. Reed, Acta Mater. 105C (2016) 449–463.
- [4] V. Velay, H. Matsumoto, V. Vidal, A. Chiba, Int. J. of Mech. Sc. 109-109 (2016) 1-13.
- [5] G. Yamane, V. Velay, V. Vidal, H. Matsumoto, Defect and Diff. Forum 385 (2018) 413-418
- [6] E. Alabort, D. Putman, R.C. Reed, Acta Mat. 95 (2015) 428-442.
- [7] J. Lin, T. Dean T, J. Mater. Process. Technol. 167 (2–3) (2005) 354-362.
- [8] H. Matsumoto, K. Yoshida, S.-H. Lee, Y. Ono, A. Chiba, Mater. Letters. 98 (2013), 209.
- [9] H. Matsumoto, L. Bin, S.-H. Lee, Y. Li, Y. Ono, A. Chiba, Metall. and Mater. Trans. A 44 (2013) 3245.
- [10] H. Imai, G. Yamane, H. Matsumoto, V. Vidal, V. Velay, Mat. Sc. And Eng. A 754 (2019) 569-580.
- [11] V. Velay, H. Matsumoto, L. Sasaki, V. Vidal, Mat.-wiss. u. Werkstofftech.45 (9) (2014) 847-853.
- [12] J. Koike, Y. Shimoyama, I. Ohnuma, R. Kainuma, K. Ishida, K. Maruyama, Acta Mater. 48 (2000) 2059–2069.